ORIGINAL PAPER

Subcutaneous injection, from birth, of epigallocatechin-3-gallate, a component of green tea, limits the onset of muscular dystrophy in *mdx* mice: a quantitative histological, immunohistochemical and electrophysiological study

Yoshiko Nakae · Katsuya Hirasaka · Junpei Goto · Takeshi Nikawa · Masayuki Shono · Mizuko Yoshida · Peter J. Stoward

Abstract Dystrophic muscles suffer from enhanced oxidative stress. We have investigated whether administration of an antioxidant, epigallocatechin-3-gallate (EGCG), a component of green tea, reduces their oxidative stress and pathophysiology in *mdx* mice, a mild phenotype model of human Duchenne-type muscular dystrophy. EGCG (5 mg/kg body weight in saline) was injected subcutaneously $4\times$ a week into the backs of C57 normal and dystrophin-deficient *mdx* mice for 8 weeks after birth. Saline was injected into normal and *mdx* controls. EGCG had almost no observable effects on normal mice or on the body weights of *mdx* mice. In contrast, it produced the following improvements in the blood chemistry, muscle histology, and electrophysiology of the treated *mdx* mice. First, the activities of serum creatine kinase were reduced to normal levels. Second, the numbers of fluorescent lipofuscin granules per unit volume of soleus and diaphragm muscles were significantly decreased by about 50% compared to the numbers in the corresponding saline-treated controls. Third, in sections of diaphragm and soleus muscles, the relative area occupied by histologically normal muscle fibres increased significantly 1.5- to 2-fold whereas the relative areas of connective tissue and necrotic muscle fibres were substantially reduced. Fourth, the times for the maximum tetanic force of soleus muscles to fall by a half increased to almost normal values. Fifth, the amount of utrophin in diaphragm muscles increased significantly by 17%, partially compensating for the lack of dystrophin expression.

Y. Nakae
Department of Oral and Maxillofacial Anatomy,
Institute of Health Biosciences,
The University of Tokushima Graduate School,
Tokushima 770-8504, Japan

K. Hirasaka · J. Goto · T. Nikawa
Department of Nutritional Physiology,
Institute of Health Biosciences,
The University of Tokushima Graduate School,
Tokushima 770-8503, Japan

M. Shono
Support Centre for Advanced Medical Sciences,
Institute of Health Biosciences,
The University of Tokushima Graduate School,
Tokushima 770-8503, Japan

M. Yoshida
Department of Degenerative Neurological Diseases,
National Institute of Neuroscience,
National Centre of Neurology and Psychiatry,
Kodaira 187-8502, Japan

P. J. Stoward
College of Life Sciences, University of Dundee,
Dundee DD1 4HN, UK

Present Address:
Y. Nakae (✉)
Laboratory of Pharmacology,
Geneva-Lausanne School of Pharmaceutical Sciences,
University of Geneva, Sciences II 4-438B,
30 Quai Ernest-Ansermet, CH-1211 Geneva 4, Switzerland
e-mail: yoshiko.nakae@ma3.seikyou.ne.jp

Introduction

Duchenne muscular dystrophy (DMD) is a human X-linked progressive muscle-wasting disease. It is caused by mutations and deletions in the dystrophin gene, resulting in the lack of full-length dystrophin molecules in the sarcolemma

(reviewed by Khurana and Davies 2003). Dystrophin stabilises the sarcolemma during muscle contraction by interacting with the intracellular actin cytoskeleton and the extracellular matrix through the dystrophin-associated glycoprotein complex in the sarcolemma (Blake et al. 2002; Dalkilic and Kunkel 2003; Ervasti 2007).

Previously, we found that dystrophin-deficient muscles of DMD patients and *mdx* mice exhibit oxidative stress because they are unable to destroy, via superoxide dismutase- and catalase-mediated pathways, all the reactive oxygen species produced from side reactions of oxygen metabolism. Thus, they suffer from more oxidative damage than age-matched normal controls, leading to the formation of end products of peroxidation such as lipofuscin and 8-oxoguanine in DNA (Nakae et al. 2001, 2004, 2005, 2006a). Many authors have attested to the role of oxidative stress in causing or modulating, for example, muscle cell atrophy, survival and regeneration (e.g. Barker and Traber 2007; Narciso et al. 2007; Zaccagnini et al. 2007). Consequently, we have hypothesized, as others have done (Disatnik et al. 1998, 2000; Rando 2002; Rando et al. 1998; Burdi et al. 2006; Dudley et al. 2006; Messina et al. 2006; Tidball and Wehling-Henricks 2007; Williams and Allen 2007), that oxidative stress is a major contributing factor in the pathology of DMD.

In this paper, we report that subcutaneous injection from birth of a low dose of the principal polyphenol antioxidant present in green tea, (−)-epigallocatechin-3-gallate (EGCG), reduces the oxidative stress in dystrophin-deficient muscles of *mdx* mice, a well-established experimental model of DMD (Bulfield et al. 1984). It also significantly improves the histology and function of their soleus and diaphragm muscles. A preliminary summary of this work has been published elsewhere (Nakae et al. 2006b, 2007). Whilst our investigation was in progress, Ruegg and his colleagues reported that feeding *mdx* mice with either a green tea extract or EGCG in food pellets improved the histological features and function of extensor digitorum longus muscle but not soleus muscle (Buetler et al. 2002; Dorchies et al. 2006).

A number of other compounds have been reported to improve the physiological function of dystrophic muscles. They include heregulin (Krag et al. 2004), L-arginine (Barton et al. 2005; Voisin et al. 2005), and the glucocorticoids methylprednisolone (Passaquin et al. 1993; Courdier-Fruh et al. 2002) and dexamethasone (Pasquini et al. 1995), all of which increase the levels of utrophin, an autosomal gene product with high homology to dystrophin (Khurana and Davies 2003; Chakkalakal et al. 2005; Hirst et al. 2005; Miura and Jasmin 2006). We have, therefore, also investigated whether EGCG administration gives rise to increased utrophin expression as this may throw additional light on the mechanisms responsible for the effects of EGCG on dystrophic muscle.

Materials and methods

EGCG treatment and tissues

All animal experiments were performed according to procedures approved by the animal care committee of the University of Tokushima Graduate School. Normal C57BL/10-SnSlc mice (abbreviated as C57 mice) and dystrophic C57BL/10-*mdx* Jic mice (abbreviated as *mdx* mice) were obtained from Japan SLC (Hamamatsu, Japan) and CLEA Japan (Tokyo, Japan), respectively. They were fed with a standard laboratory diet (CE-2; CLEA Japan) and given free access to tap water, and housed in a room with 12 h light/dark cycles at 22–23°C. Males and females of the same strain were mated at the age of 10 weeks. Littermate neonates were divided into two groups, a test and a control group. (−)-Epigallocatechin-3-gallate (EGCG; purity ≥ 95%), extracted from green tea, was purchased from Sigma-Aldrich Japan, Tokyo, and dissolved in sterile physiological saline (Otuka Pharmaceutical, Tokushima, Japan) at a concentration of 0.4 mg/ml, filtered through a sterile syringe with a 0.20 μm pore filter (DISMIC-13cp; Advantec Toyo, Tokyo, Japan), stored at 4°C, and used within 10 days after preparation. Calculated volumes of the filtered EGCG solution, corresponding to a dose of 5 mg EGCG/kg body weight, were injected subcutaneously, using either autoclaved microsyringes (Hamilton, Reno, Nevada, USA) or sterile disposable syringes into the backs of both *mdx* and normal C57 mice, 4× a week for 8 weeks from either the day of birth or a day after birth. As controls, *mdx* and normal mice were injected with physiological saline only. At the end of the treatment schedule, all mice were sacrificed by cervical dislocation. Their diaphragm, soleus and lingual muscles, livers and kidneys were removed. The total numbers of mice used in the present study were 8♂, 13♀: C57 + saline; 13♂, 15♀: C57 + EGCG; 9♂, 9♀: *mdx* + saline; 8♂, 11♀: *mdx* + EGCG.

Serum creatine kinase (CK) activity

Blood samples were taken from the hearts of 8-week-old mice under chloroform anaesthesia and centrifuged at 3,000 rpm for 10 min to obtain sera. The activities of muscle-derived CK in the test and control samples were measured simultaneously at 37°C by Mitsubishikagaku Biochemical Laboratories (Tokyo, Japan) using a routine UV-method (Gerhardt and Wulff 1983) and commercial kit (CicaLiquid CK; Kanto Chemical, Tokyo, Japan), with creatine phosphate as the substrate. The numbers of mice used for the activity measurements were 3♂, 1♀: C57 + saline; 3♂, 3♀: C57 + EGCG; 4♂, 3♀: *mdx* + saline; 5♂, 4♀: *mdx* + EGCG.

Oxidative stress

The levels of oxidative stress in three untreated and three treated male *mdx* mice were determined by counting the number of autofluorescent lipofuscin granules or clumps accumulated focally in frozen, 7 μm-thick, cross-sections of diaphragm and soleus muscles as described previously (Nakae et al. 2004). Optical slices of each section excited simultaneously at 488 and 568 nm were captured at 16 consecutive confocal planes using a confocal laser-scanning microscope (TCS NT; Leica, Heidelberg, Germany) and used to reconstruct a fluorescent image of the section. Assuming that the thickness of the sections was uniformly 7 μm, the numbers of lipofuscin granules or clumps per mm^3 were calculated. The muscles of the normal mice controls were not examined as previously we found that their lipofuscin content was negligible (Nakae et al. 2004).

Histology

Frozen transverse sections, 7 μm thick, of diaphragm and soleus muscles, tongue, liver and kidney were prepared as described previously (Nakae et al. 2004). The sections were fixed in 1:1 v/v acetone–methanol at 4°C for 5 min, stained with Haematoxylin solution (DakoCytomation, Kyoto, Japan) followed by 0.25% Eosin Y (Merck, Tokyo, Japan) in 79% ethanol containing 0.5% acetic acid, and mounted in Histomount (Zymed Laboratories, South San Francisco, California, USA). Images of the sections were captured under a Zeiss Axioskop microscope (Oberkochen, Germany) fitted with a Fujix digital camera (HC-2500 3CCD; Fuji Photo Film, Tokyo, Japan) using Photograb-2500 version 1.0 software (Fuji Photo Film).

The total areas occupied respectively by mature muscle fibres with peripheral nuclei (i.e. histologically normal fibres), muscle fibres with central nuclei (regenerating muscle fibres), and necrotic muscle fibres, were measured in sections of soleus and diaphragm muscles using a personal computer and ImageJ version 1.37v software (NIH, Bethesda, Maryland, USA). The necrotic fibres were identified as degenerated fibres with diffusely-stained eosinophilic myofibrils and broken sarcolemmas, and were often associated with macrophages. The total tissue areas of each section were also measured. The total area of connective tissue in each section was calculated by subtracting the sum of the areas of the three muscle fibre forms from the total tissue section areas. The relative areas of the muscle fibre forms and connective tissue were expressed as percentages of the total tissue area. The total observed cross-section areas of diaphragm muscle were 1.79×10^{-2} cm^2 in *mdx* + saline ♂ mice (*n* = 3) and 2.13×10^{-2} cm^2 in *mdx* + EGCG ♂ (*n* = 3) mice. The corresponding areas in soleus muscle were 2.81×10^{-2} and 3.10×10^{-2} cm^2, respectively.

Contraction recording and analysis

Freshly dissected soleus muscle was stimulated directly by an electrical field generated between two parallel electrodes connected to a stimulator SEN-3201 and bath drive amplifier SEG-3101 (Nihon Kohden, Tokyo, Japan), according to the method of Xiao et al. (2000) with modifications. The muscle length was adjusted until a single stimulus pulse or a train of pulses elicited the maximum force during a twitch or tetanus under isometric conditions. Rectangular pulses [0.5 ms delay, 0.5 ms duration, 500 ms interval time (2 Hz) and 4 V] were applied to elicit twitch contractions for 2 min. The interval time was then changed to 50 ms (20 Hz) to elicit fused contractions (complete tetanus).

All experiments were performed at 37°C. The tetanic force (muscle contraction) was recorded as a function of time in a physiological solution (5 mM HEPES buffer, pH 7.4, containing 150 mM NaCl, 4 mM KCl, 1.8 mM CaCl$_2$, 1 mM MgCl$_2$ and 5.6 mM glucose) in a magnus tube (Kishimoto Medical Instruments, Kyoto, Japan). A personal computer (Macintosh Server G3; Apple Japan, Tokyo, Japan), digital chart recorder MacLab 8e (Bio Research Centre, Nagoya, Japan), transducer UM-203 and detector AP-5 (Kishimoto Medical Instruments) were used for data acquisition. The data were analysed using MacLab Chart version 3.5.2/s software (Bio Research Centre). The specific tetanic force was determined as the maximal force per cross sectional area (CSA). The CSA was calculated from the wet weight and length of the muscle assuming a muscle density of 1.056 g/cm^3. The mean time ($T_{1/2max}$) from when the tetanic force first reaches a maximum to when the force falls by a half was determined from the tetanic force–contraction time curves. The numbers of mice used in the contraction analyses were 6♂, 0♀ C57 + saline; 6♂, 1♀ C57 + EGCG; 6♂, 2♀ *mdx* + saline; 7♂, 2♀ *mdx* + EGCG.

Utrophin immunohistochemistry

Frozen sections, 7 μm thick, of diaphragm and lingual muscles were cut and fixed in 1:1 v/v acetone–methanol at 4°C for 5 min. The sections were first blocked at room temperature for 1 h in 0.01 M phosphate-buffered saline, pH 7.4, containing 5% goat normal serum (G-9023; Sigma-Aldrich Japan) (PBSS). They were incubated overnight at 4°C with rabbit anti-utrophin antibody (1: 200; H-300; Santa Cruz Biotechnology, Santa Cruz, California, USA) in PBSS, followed by incubation at room temperature for 2 h with goat anti-rabbit IgG conjugated with Alexa Fluor 568 (1: 1,000; Molecular Probes, Eugene, Oregon, USA). The sections

were mounted in Vectashield mounting medium (Vector Laboratories, Burlingame, California, USA) and sealed with nail varnish. Fluorescence images of the immuno-stained tissues excited at 568 nm were captured using a confocal laser-scanning microscope as described previously. Cell nuclei in some sections immunostained for utrophin were subsequently labelled for 30 min with 1 μg/ml Hoechst 33258 (Nacalai Tesque, Kyoto, Japan) in 0.1 M Tris–HCl buffer, pH 7.4 (Nakae et al. 2001). These sections were also mounted in Vectashield mounting medium and sealed with nail varnish. Fluorescence images of the double-labelled sections excited simultaneously at 408 and 543 nm were captured in a Nikon confocal laser-scanning microscope (C1si; Tokyo, Japan). All fluorescence images were reconstructed from a stack of 16 consecutive confocal planes (z-stack).

Quantitative determination of utrophin expression using Western blotting

Diaphragm muscles were removed from three mice from the C57 + saline group, three from the C57 + EGCG group, four from the *mdx* + saline group and four from the *mdx* + EGCG group. Each diaphragm muscle was quenched immediately in a microtube cooled with liquid nitrogen and stored at −80°C until use. The frozen muscle was ground to a powder in liquid nitrogen in a mortar. The tissue powder was homogenised in ice-cold PRO-PREP (iNtRON Biotechnology, Sungnam, Korea) using a Polytron (RT1300D; Kinematica AG, Littau, Switzerland) and centrifuged at 13,000 rpm at 4°C for 5 min. The supernatants were used for Western blotting after determining their protein concentrations with the Lowry method (Dc Protein Assay Kit; BIO-RAD Laboratories, Hercules, California, USA). SDS-gel electrophoresis followed by blotting to PVDF membranes (Invitrolon PVDF; Invitrogen, Carlsbad, California, USA) was performed with NuPAGE kits (Invitrogen), with a small modification, according to the manufacturer's instructions. Eighteen microgram of total protein was loaded to each gel well in 3–8% SDS-polyacrylamide gel (NuPAGE Tris–Acetate Gel; Invitrogen). A molecular weight marker (HiMark HMW Standard; Invitrogen) was also loaded. After electrophoresis, the gel film was cut into two halves. One half was used for quantifying the relative amount of protein loaded in each well by staining with Coomassie Brilliant Blue G-250 (SimplyBlue SafeStain; Invitrogen). The other half was used for immunoblotting for utrophin. Proteins in the half-gel film were blotted to PVDF membrane. The membrane was first blocked at room temperature for 4 h in 5% skim milk (ECL Advance Western Blotting Detection Kit; Amersham Biosciences, Buckinghamshire, UK) in 0.01 M phosphate-buffered saline, pH 7.4, containing 0.1% Tween-20 (for molecular biology;

Sigma-Aldrich) (PBST), and then incubated overnight at 4°C with rabbit anti-utrophin antibody (1: 500; H-300; Santa Cruz Biotechnology) and subsequently with goat anti-rabbit IgG conjugated with horseradish peroxidase at room temperature for 1 h (ECL Plus Western Blotting Reagent Pack; Amersham Biosciences). After rinsing the PVDF membrane thoroughly in PBST, the utrophin immuno-complex was detected with a substrate for chemoluminescence (Lumigen TMA-6; Amersham Biosciences). The protein bands in all electrophoretic and immunoblotting patterns were quantified using a personal computer and ImageJ version 1.34s software (NIH) and KaleidaGraph version 3.6.3 software (Hulinks, Tokyo, Japan).

Quantitative determination of utrophin mRNA using real-time RT-PCR

Diaphragm muscles were removed from three C57 + saline mice, three mice from the C57 + EGCG group, four from the *mdx* + saline group and four from the *mdx* + EGCG group. They were quenched as described for Western blotting in the previous paragraph and stored at −80°C until use. Using the RNeasy Fibrous Tissue Mini Kit (Qiagen, Tokyo, Japan), total RNA was extracted from the powder of the tissue prepared as described for Western blotting and stored at −80°C. cDNA was prepared by reverse transcription (RT) using the total RNA, random hexamers and the GeneAmp RNA PCR kit (Applied Biosystems, Foster City, California, USA). The reaction mixture was incubated at 45°C for 15 min, then 99°C for 5 min, and finally at 5°C for 5 min and stored at −80°C before use. Polymerase chain reactions (PCR) were carried out in a real-time PCR system (7500; Applied Biosystems) using a reverse transcription mixture containing cDNA, a utrophin primer (Mm00810176(s1; Applied Biosystems), a ribosomal protein S18 primer (Mm00507222(s1; Applied Biosystems) as an endogenous control, and TaqMan Universal PCR Master Mix (Applied Biosystems), according to the manufacturer's instructions. First, uracil *N*-glycosylase contained in the reaction mixture was activated at 50°C for 2 min. Then, AmpliTaq Gold activation and denaturation of uracil *N*-glycosylase was carried out by incubating the mixture at 95°C for 10 min. Each 40 cycles consisted of denaturation at 95°C for 15 s and annealing and extension of the primer at 60°C for 1 min. No PCR products were detected in the negative controls of the amplification in which the reverse transcription mixtures were replaced with RNase-free water. The relative amounts of utrophin and ribosomal protein S18 transcripts were determined in the linear ranges of amplifications. The relative amount of utrophin mRNA was expressed as the ratio of the relative amount of utrophin transcripts to that of ribosomal protein S18 transcripts, in the same sample. The RT-PCR was repeated 2–3× for each sample.

Statistical analyses

Data were expressed as means ± SEM. Student's *t* test was used to test statistical significances between two means. The data for four groups were also subjected to Bonferroni's and Scheffe's multiple *t* tests using SPSS software. Significance levels obtained with Student's, Bonferroni's and Scheffe's tests are denoted by the symbols P, P_B and P_S, respectively. They were considered significant at $P < 0.05$.

Results

Effects of EGCG treatment on body weights

The EGCG treatment had no significant effects on the mean body weights of either normal ($P > 0.1$, $P_B > 0.9$, $P_S > 0.5$) or *mdx* mice ($P > 0.9$, $P_B > 0.9$, $P_S > 0.6$) compared to the corresponding controls injected with saline (Fig. 1). The mean body weight of male mice was 3.9–5.3 g higher than that of female mice in each experimental group ($P < 0.01$).

Effects of EGCG treatment on serum creatine kinase activities

As shown in Fig. 2, the mean activity of serum creatine kinase in 8-week-old *mdx* control mice (23,315 ± 2,845 IU/l) was about 21× higher than that of age-matched C57 normal control mice (1,125 ± 406 IU/l).
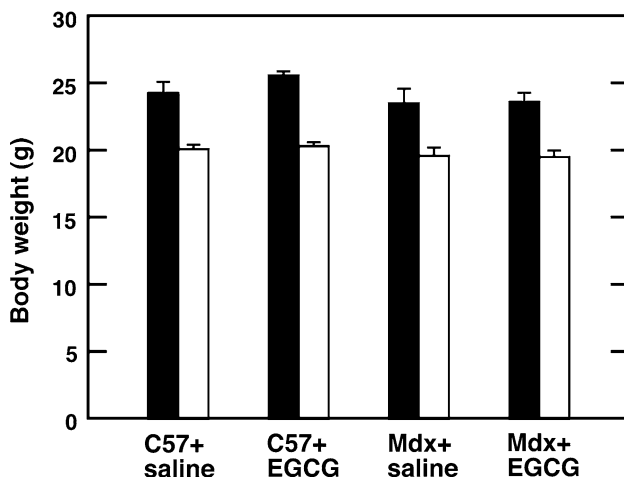

Fig. 1 Mean body weights (*columns*) and SEMs (*bars*) of 8-week-old mice after continuous treatment with EGCG or saline from birth (*n* = 8–15). The differences of the mean weights between the saline and EGCG treatments are not significant for either males (*black columns*) or females (*white columns*) of *mdx* ($P > 0.9$, $P_B > 0.9$, $P_S > 0.6$) and C57 normal ($P > 0.1$, $P_B > 0.9$, $P_S > 0.5$) mice. However, the differences between males and females in each experimental group are significant ($P < 0.01$)
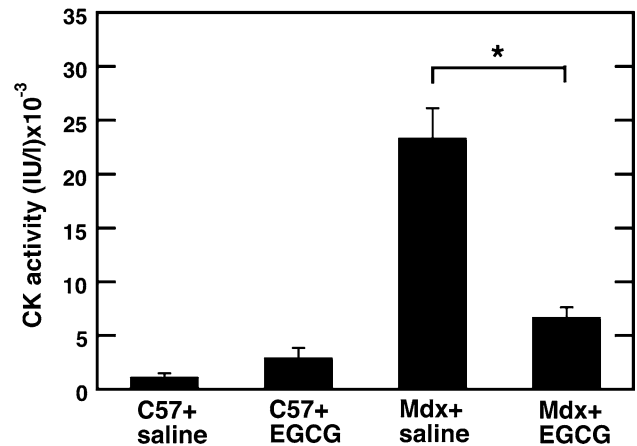

Fig. 2 Mean serum creatine kinase (CK) activities (*columns*) and SEMs (*bars*) of 8-week-old *mdx* and C57 normal mice after continuous treatment with saline or EGCG from birth. EGCG treatment reduces the initial, very high mean activity in *mdx* mice, 21× that of normal C57 control mice, by about 75%, close to the level of EGCG-treated normal mice. EGCG does not significantly alter the low activity in normal mice. * $P < 0.001$, * $P_B < 0.001$, * $P_S < 0.001$

EGCG injection into *mdx* mice after birth significantly reduced the activity by about 75% ($P < 0.001$, $P_B < 0.001$, $P_S < 0.001$). The mean activity (6,670 ± 996 IU/l) was similar to, and not significantly different from ($P > 0.1$, $P_B > 0.5$, $P_S > 0.3$), that of the normal mice treated with EGCG (2,895 ± 994 IU/l). However, EGCG had no significant effect on the activity in normal C57 mice ($P > 0.2$, $P_B > 0.9$, $P_S > 0.9$).

Effects of EGCG treatment on muscle oxidative stress and histology

The effects of EGCG treatment on the accumulation of an oxidative stress marker, lipofuscin, in diaphragm and soleus muscles are illustrated in Fig. 3. This shows qualitatively that the number of yellow or orange fluorescent lipofuscin granules in both muscles is noticeably much less compared to those in untreated *mdx* controls. Quantitatively, the mean numbers of lipofuscin granules or clumps per unit volume of tissue were reduced significantly by 53% ($P < 0.005$) and 41% ($P < 0.05$) in diaphragm and soleus muscles, respectively (Fig. 4).

The typical histological appearances of diaphragm and soleus muscles in 8-week-old *mdx* mice treated with saline alone compared to those of *mdx* mice given EGCG are shown in Fig. 5a, b (diaphragm) and Fig. 5c, d (soleus), respectively. Qualitatively, fewer necrotic muscle fibres and less connective tissue were seen in the muscles of treated mice compared to those seen in control mice. In contrast, there were more histologically normal muscle fibres. Quantitatively, the EGCG treatment reduced the

Fig. 3 *Upper figure*: confocal fluorescence images of sections of *mdx* diaphragm (**a**) and soleus (**c**) muscles containing numerous yellow or orange autofluorescent lipofuscin (LF) granules after treatment with saline compared to their sparsity in the corresponding muscles after EGCG treatment (*lower figure*, **b**, **d** for diaphragm and soleus, respectively). *Bars* = 50 μm
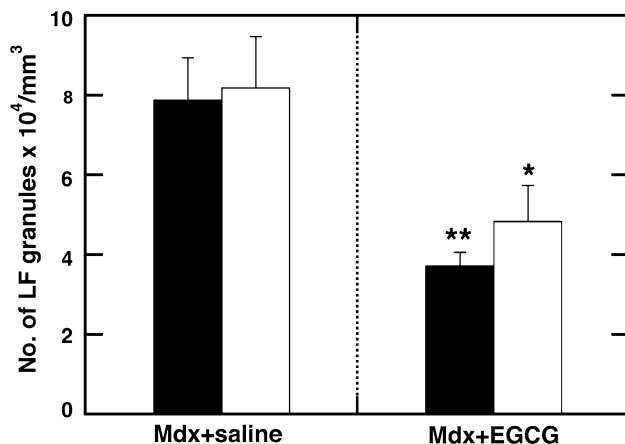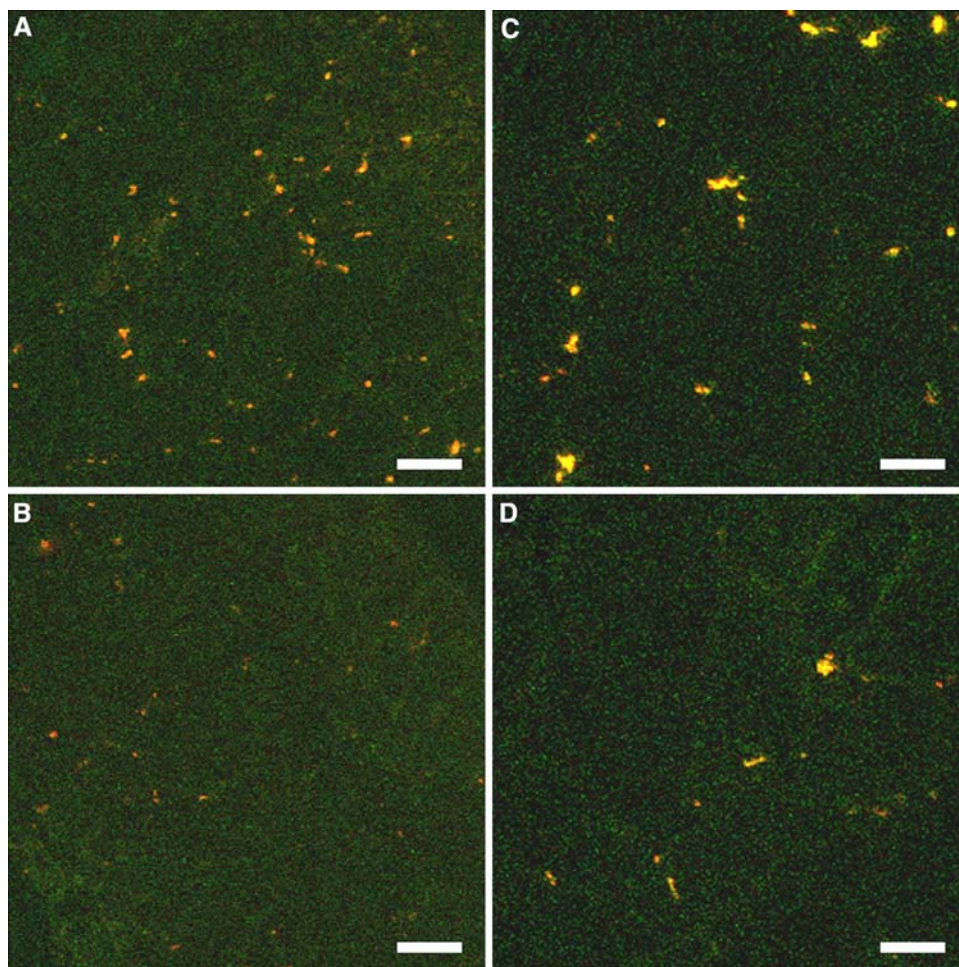

Fig. 4 Mean numbers (*columns*) ± SEMs (*bars*) of lipofuscin granules or clumps per unit volume in diaphragm (*black columns*) and soleus muscles (*white columns*) in *mdx* mice treated with saline or EGCG for 8 weeks after birth. The EGCG treatment reduced the numbers by 53 and 41% in diaphragm and soleus muscles, respectively. * $P < 0.05$, ** $P < 0.005$ versus control values

relative area occupied by necrotic tissue but increased that of histologically normal muscle fibres. These changes are shown quantitatively in Fig. 6. In *mdx* diaphragm muscles,

EGCG increased the mean relative area occupied by histologically normal muscle fibres almost 2-fold from $24.7 \pm 2.0\%$ to $46.9 \pm 5.1\%$ ($P < 0.01$) compared to that in saline-treated *mdx* mice but reduced the relative areas of connective tissue by 41%, from $37.2 \pm 3.6\%$ to $22.1 \pm 1.9\%$ ($P < 0.01$), and of necrotic muscle fibres by 93%, from $9.6 \pm 3.7\%$ to $0.7 \pm 0.2\%$ ($P < 0.05$). In contrast, the relative percentage areas of muscle fibres with central nuclei showed no significant change ($P > 0.8$) between control ($28.5 \pm 5.8\%$) and EGCG-treated samples ($30.4 \pm 4.9\%$). In *mdx* soleus muscles, EGCG treatment led to a 1.5-fold increase in the mean relative area of histologically normal muscle fibres from $20.8 \pm 3.5\%$ to $31.2 \pm 1.8\%$ ($P < 0.05$) but reduced the areas occupied by necrotic muscle fibres by 95% from $15.3 \pm 4.7\%$ to $0.740 \pm 0.575\%$ ($P < 0.01$). However, the relative percentage areas occupied by regenerating or regenerated muscle fibres with central nuclei showed no significant changes ($P > 0.05$) between control ($40.3 \pm 6.8\%$) and test samples ($49.1 \pm 3.2\%$). Similarly, the relative areas of connective tissue were not significantly different ($P > 0.05$) in control ($23.6 \pm 4.6\%$) and test samples ($18.9 \pm 2.5\%$).
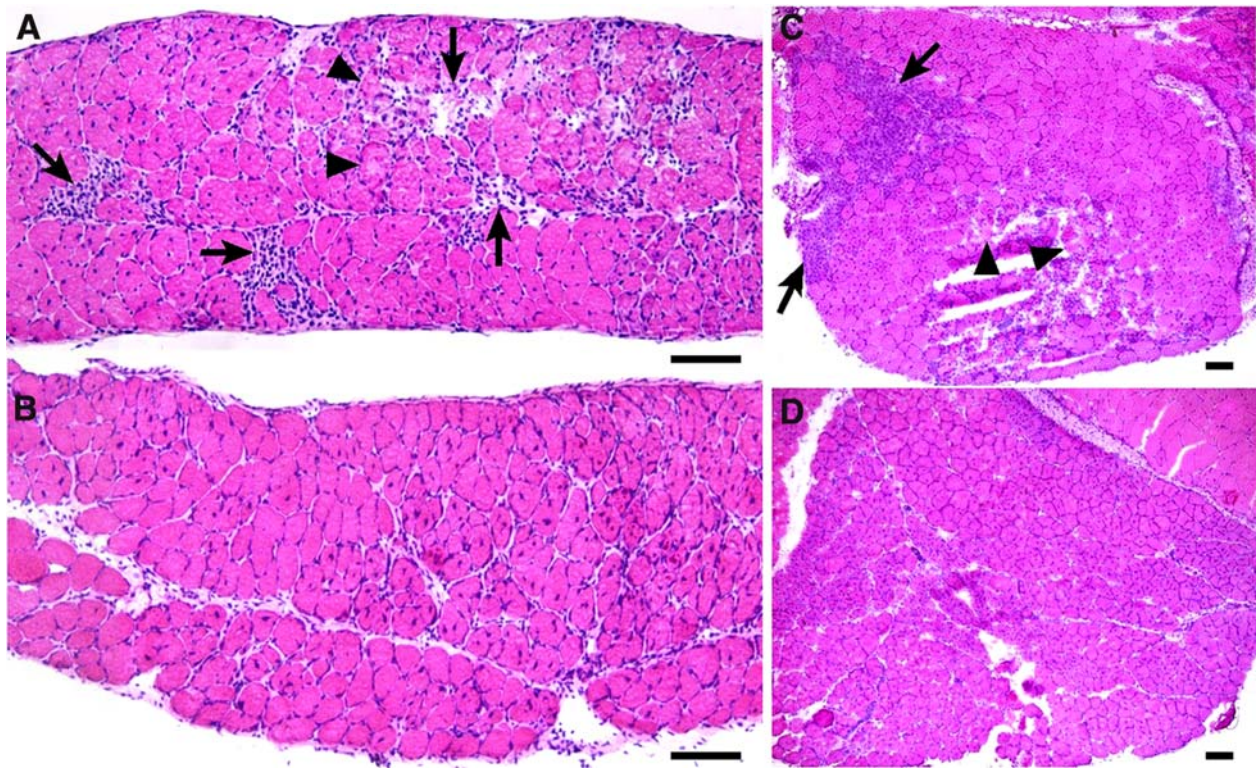
Fig. 5 Histology of diaphragm muscles of 8-week-old *mdx* mice without (**a**) and after (**b**) EGCG treatment, and of soleus in untreated (**c**) and treated (**d**) *mdx* mice. The untreated mice received saline only. Haematoxylin and eosin. Note the change towards normal histology in both muscles of the EGCG-treated mice: there is much less muscle necrosis (*arrowheads*) and replacement by connective tissue (*arrows*) in the EGCG-treated mice (**b**, **d**) compared to that seen in the corresponding muscles of the saline-treated *mdx* mice (**a**, **c**). *Bars* = 100 μm
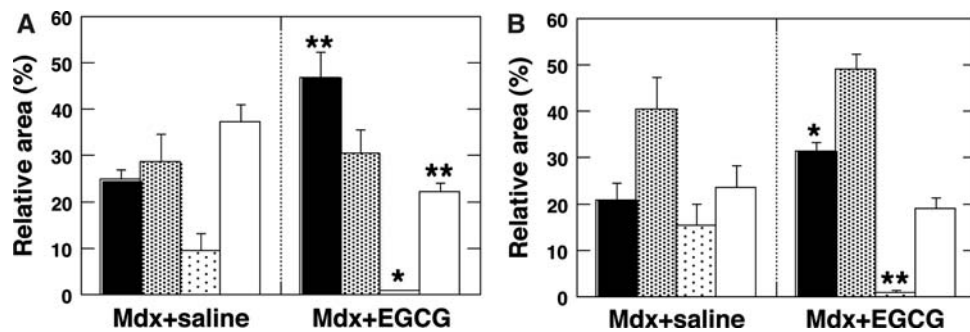

Fig. 6 Quantitative changes in the histology of diaphragm (**a**) and soleus (**b**) muscles of 8-week-old *mdx* mice after EGCG treatment. The columns are the mean relative areas (expressed as percentages of the total observed cross-section area) occupied by histologically normal fibres (*black columns*), muscle fibres containing central nuclei (*grey columns*), necrotic muscle fibres (*dotted columns*) and connective tissue (*white columns*). The *bars* are SEMs. In the diaphragm muscles of EGCG-treated mice, the mean normal muscle fibre area increases about two-fold but the connective tissue and necrotic muscle areas are significantly reduced by about 41 and 93%, respectively, compared to those in the corresponding saline-treated controls (**a**). However, the mean percentage area of muscle fibres with central nuclei is not significantly altered. * $P < 0.05$, ** $P < 0.01$ versus control values. In soleus muscles of EGCG-treated *mdx* mice, the mean normal muscle area increases about 1.5-fold but the necrotic muscle fibre area decreases by 95%, compared to those in the corresponding saline-treated controls (**b**). Both changes are significant. In contrast, there is no significant change in the mean percentage areas of muscle fibres with central nuclei and the connective tissue. * $P < 0.05$, ** $P < 0.01$ versus control values

There were no observable effects on the histology of liver and kidney at the light microscopical level after EGCG treatment in either 8-week-old *mdx* mice or C57 normal mice.

Effects of EGCG treatment on muscle contraction

The mean maximum isometric tetanic force (0.49 ± 0.12 N/cm^2) and $T_{1/2max}$ (50 ± 13 s), the mean time

for this force to fall by a half, for soleus muscles of saline-treated 8-week-old *mdx* mice were, respectively, 31% ($P < 0.001$, $P_B < 0.01$, $P_S < 0.009$) and 48% ($P < 0.01$, $P_B < 0.01$, $P_S < 0.009$) of those of age-matched normal controls (1.6 ± 0.3 N/cm^2, 103 ± 9 s) (Fig. 7). EGCG treatment for 8 weeks after birth did not significantly affect the mean maximum intensities of the specific isometric tetanic force of *mdx* soleus muscles showing the mean value 0.79 ± 0.19 N/cm^2 ($P > 0.2$, $P_B > 0.9$, $P_S > 0.7$). In contrast, $T_{1/2max}$ of *mdx* muscles increased 1.9-fold (94 ± 7 s) ($P < 0.01$, $P_B < 0.01$, $P_S < 0.02$), reaching almost the level of EGCG-treated normal mice (101 ± 8 sec). EGCG treatment did not significantly alter the isometric contraction of normal soleus muscle ($P > 0.5$, $P_B > 0.9$, $P_S > 0.8$).

Effects of EGCG treatment on utrophin expression

In the diaphragm muscles of 8-week-old normal mice injected with physiological saline, utrophin was mostly localised in neuromuscular junctions, blood vessels and peripheral nerves (Fig. 8a–c). None was observed in the extrasynaptic sarcolemma. In contrast, in age-matched *mdx* diaphragm muscles from saline-treated controls, utrophin was localised predominantly on the extrasynaptic sarcolemma along the entire length of immature central-nucle-

ated basophilic myofibres (Fig. 8d–g). As these cells matured, utrophin gradually decreased and disappeared on the extrasynaptic sarcolemma (Fig. 8d–g). However, EGCG treatment of *mdx* mice increased the amount of utrophin on the extrasynaptic sarcolemma not only in immature muscle cells but also in mature muscle cells (Fig. 8h–j).

In lingual muscles, unlike the changes observed in diaphragm muscles, very few regenerated muscle fibres with central nuclei were seen in *mdx* mice treated with either EGCG or physiological saline (Fig. 9c, g). Necrotic lesions were also rarely observed. EGCG treatment elevated utrophin levels on the extrasynaptic sarcolemma along the entire length of *mdx* lingual muscle fibres (Fig. 9). Utrophin expression in blood vessels, nerve fibres and stratified squamous epithelia in the lingual muscle of *mdx* mice also increased after EGCG treatment.

Quantification of the expression bands of full-length utrophin (identified as the 395 kDa protein) obtained after typical SDS-gel electrophoresis and Western blotting of diaphragm extracts are shown in Fig. 10. The mean amount of utrophin formed was significantly higher by 18% in *mdx* control diaphragm muscles than in C57 controls ($P < 0.001$, $P_B < 0.005$, $P_S < 0.006$). The EGCG treatment resulted in a significant increase of utrophin over these base levels by 17% ($P < 0.01$, $P_B < 0.003$, $P_S < 0.004$) and 14% ($P < 0.01$, $P_B < 0.02$, $P_S < 0.03$) in *mdx* and C57 diaphragm muscles, respectively (Fig. 10).
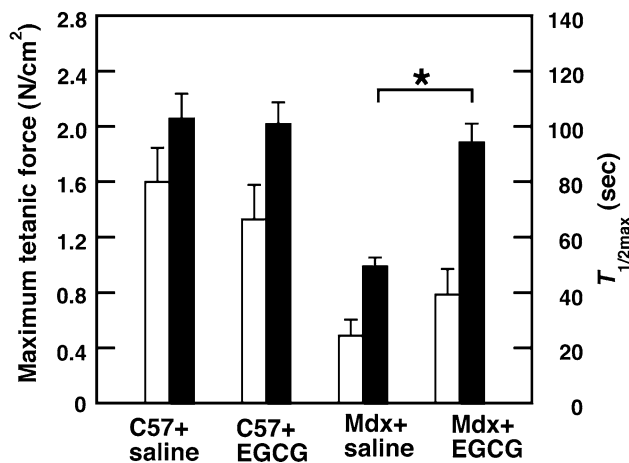
Effects of EGCG treatment on utrophin mRNA expression

Figure 10 also shows the effects of the EGCG treatment on the relative expression of mRNA determined as ratios of utrophin mRNA/ribosomal protein S18 mRNA as an endogenous control. The mean relative expression of utrophin mRNA in diaphragm muscles ranged from 0.748 to 0.913 in the test and control groups of *mdx* and normal mice, but the effects of EGCG were not significant in *mdx* ($P > 0.9$, $P_B > 0.9$, $P_S > 0.9$) or normal C57 ($P > 0.2$, $P_B > 0.9$, $P_S > 0.6$) muscles.

Discussion

When the principal active component of green tea, epigallo-catechin-3-gallate (EGCG) is injected $4\times$ a week from birth at a dose of 5 mg/kg body weight for 8 weeks into either normal or *mdx* mice, it has neither any effect on their body weights (Fig. 1), in agreement with previous reports (Goodin and Rosengren 2003; Dorchies et al. 2006), nor any effect on the histology of their livers and kidneys, indicating that it is not toxic at this dosage. However, when administered in this way, EGCG limits, and possibly delays, the onset of pathological damage in the muscles of
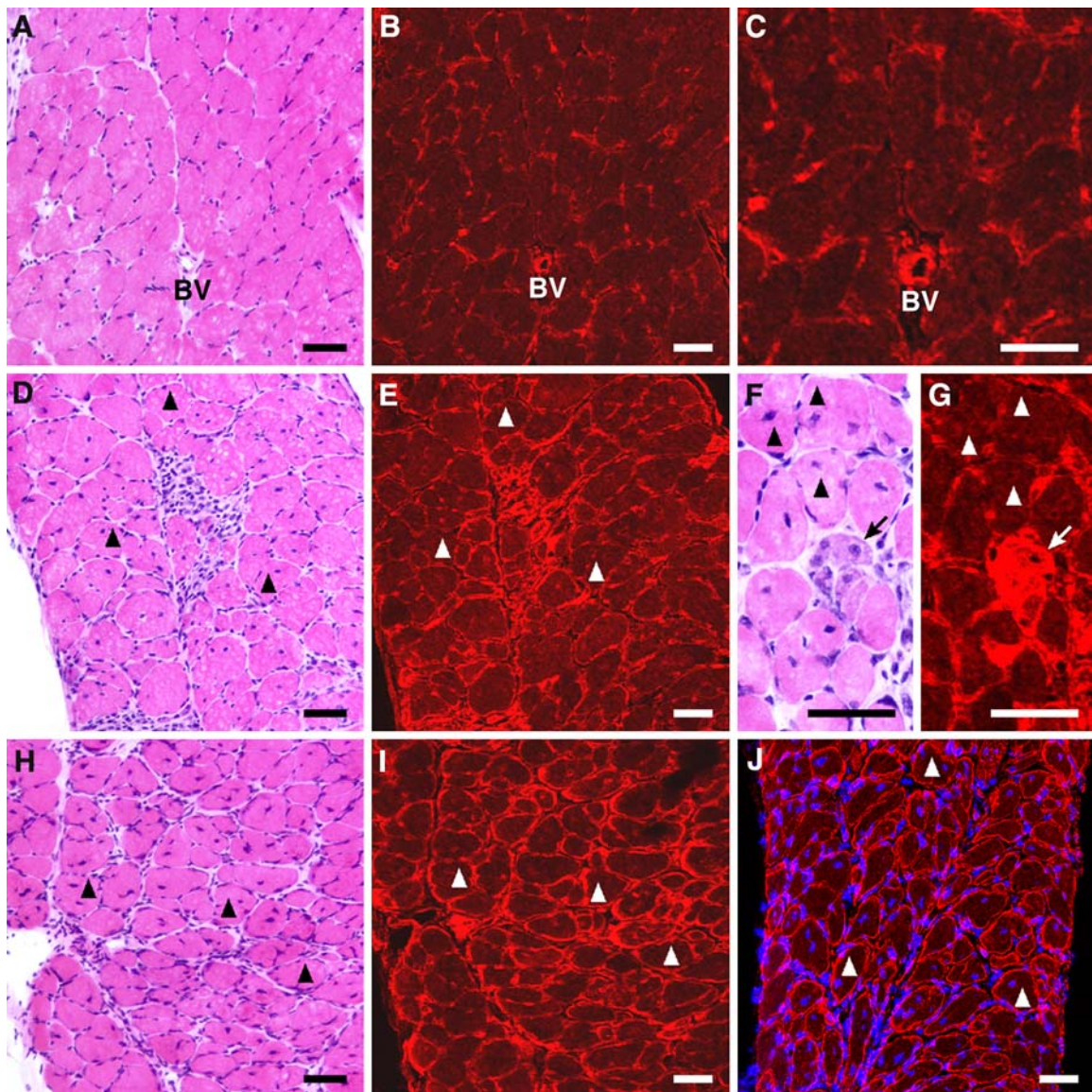

Fig. 7 Isometric tetanic contractions of soleus muscles of C57 and *mdx* mice treated continuously with saline (controls) or EGCG for 8 weeks after birth. Each *column* and *bar* is the mean and SEM, respectively. The mean maximum specific tetanic force (*white columns*) and $T_{1/2max}$, the mean time for this force to fall by a half (*black columns*), of isolated soleus muscles from saline-treated *mdx* control mice were less than half of those of corresponding age-matched C57 normal controls. The EGCG treatment significantly increased $T_{1/2max}$ of *mdx* soleus muscles 1.9-fold to almost the level of normal mice treated with EGCG, but did not significantly increase the maximum tetanic force. EGCG did not significantly affect the function of normal C57 soleus muscles ($P > 0.5$, $P_B > 0.9$, $P_S > 0.8$). * $P < 0.01$, * $P_B < 0.01$, * $P_S < 0.02$

Fig. 8 Increase in the level of extrasynaptic sarcolemmal utrophin in diaphragm muscles of 8-week-old *mdx* mice treated with EGCG for 8 weeks. **a**–**c** C57 + saline. **d**–**g** *Mdx* + saline. **h**–**j** *Mdx* + EGCG. **b**, **e**, **i** Confocal fluorescence images showing utrophin localisation compared to serial cross-sections stained with haematoxylin and eosin (**a**, **d** and **h**, respectively). **c** Higher magnification image of **b**. **f**, **g** Higher magnifications of another area in the same section as **d** and **e**, respectively. **j** Confocal image of a serial section double-stained for utrophin and cell nuclei. In C57 normal muscles, most utrophin seems to be present at neuromuscular junctions on the sarcolemma of muscle fibres (**b**, **c**). Blood vessels (*BV* in **a**–**c**) also contain utrophin. In *mdx* saline-treated control muscle, utrophin is abundantly localised on the sarcolemma along the entire length in regenerating immature muscle cells (*arrows* in **f**, **g**) with central nuclei and basophilic cytoplasm but disappears as the muscle cells mature (*arrowheads* in **d**–**g**). EGCG treatment of *mdx* mice enhances the extrasynaptic sarcolemmal level of utrophin in mature muscle fibres (*arrowheads* in **h**–**j**). Compare with Fig. 9. *Bars* = 50 μm

mdx mice as shown by the following findings reported here. First, the activity of serum creatine kinase, a marker of sarcolemmal damage, is reduced to almost normal levels (Fig. 2). Second, oxidative stress in muscle fibres is reduced as shown by the approximately 50% decrease in the number of lipofuscin granules that are formed (Figs. 3, 4). Third, the histology of both the fast-contracting diaphragm muscle and the slow-contracting soleus is improved and closely resembles that of normal muscle

(Figs. 5, 6). Fourth, the mean time for the maximum tetanic force to fall by a half ($T_{1/2max}$) increases in *mdx* soleus muscles to an almost normal level (Fig. 7). Fifth, the amount of utrophin formed in *mdx* diaphragm muscle is significantly increased by 17% (Figs. 8–10).

Our finding of a significantly lower number of lipofuscin granules in the muscles of EGCG-treated *mdx* mice substantiates our working hypothesis proposed earlier (Nakae et al. 2004) that administration of an antioxidant such as
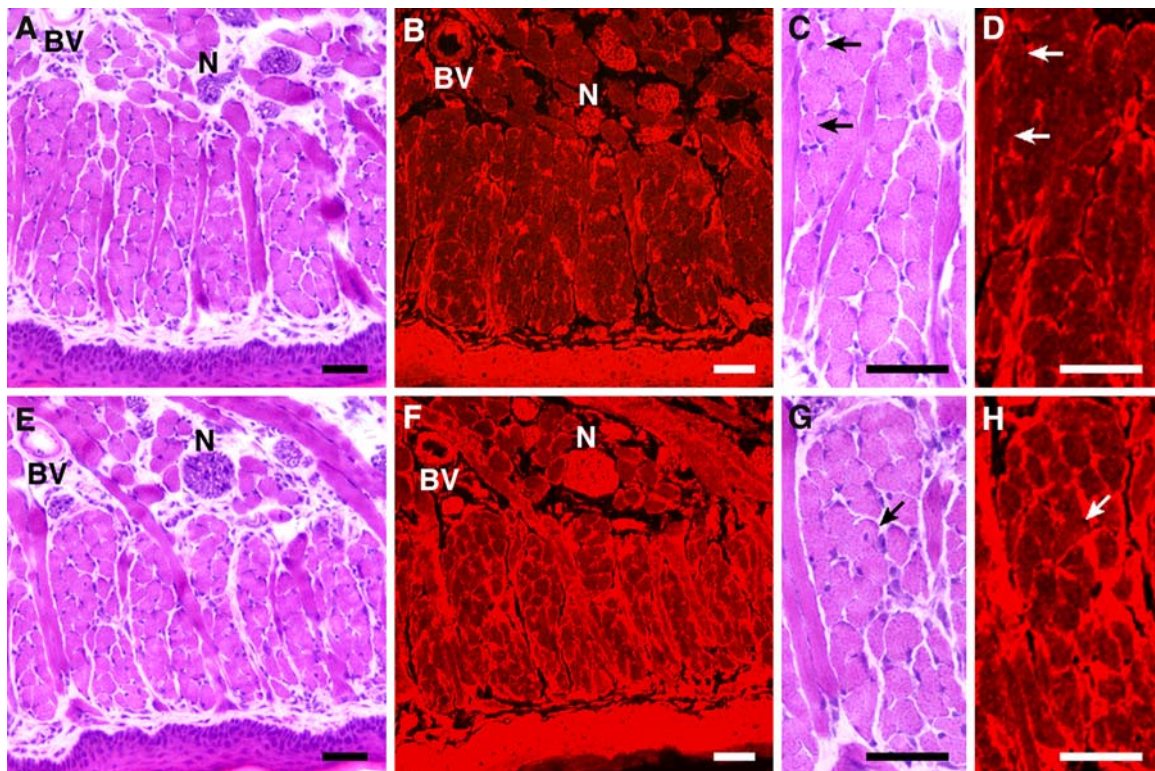
Fig. 9 Increase in the extrasynaptic sarcolemmal level of utrophin in lingual muscles in 8-week-old *mdx* mice after treatment with EGCG from birth. **a–d** *Mdx* + saline. **e–h** *Mdx* + EGCG. **b**, **d**, **f**, **h** Confocal images of serial cross-sections immunostained for utrophin, corresponding to the serial sections stained with haematoxylin and eosin shown in **a**, **c**, **e**, and **g**, respectively. Necrotic lesions are sparse in lingual muscles of *mdx* mice treated with either saline or EGCG; regenerating muscle cells with central nuclei are rarely seen (*arrows* in **c**, **d**, **g**, **h**). Interestingly, the EGCG treatment results in an enhanced extrasynaptic level of utrophin in *mdx* lingual muscles showing no serious dystrophic damage. More utrophin is also present in blood vessels (*BV*), peripheral nerves (*N* in **b**, **f**) and stratified squamous epithelia in the tongues of EGCG-treated mice (**f**) than in saline-treated controls (**b**). *Bars* = 50 μm

EGCG can protect muscle fibres from oxidative stress, but for how long this protection can be maintained has still to be established.

Other reports (e.g. Messina et al. 2006; Burdi et al. 2006) of improvements in muscle function and histopathology in *mdx* mice treated with other antioxidants, such as IRFI-042 or BN 82270, support our findings. Both EGCG (Fig. 2) and IRFI-042 reduce the mean activity of serum creatine kinase by about 75% in *mdx* mice. This lowering is greater than the reductions observed after heregulin (about 50%, Krag et al. 2004) or ʟ-arginine (about 60%, Voisin et al. 2005) administration reported previously. That the reduction of creatine kinase activity in our investigation after EGCG treatment is not due to the inhibition of the activity by EGCG is confirmed by the non-significant difference between the activities in normal mice injected with EGCG and those given saline only (Fig. 2).

The weekly dosage of EGCG administered in our investigation was 20 mg/kg body weight, equivalent to an average daily dosage of 2.86 mg/kg body weight. This is much less than the intraperitoneal dosage of 25 mg/kg body weight administered every day for 1 week by Goodin and Rosengren (2003), who showed that EGCG had no toxic effects in mice. It is also considerably lower than the average dosage of 150 mg EGCG/kg body weight per day consumed in food pellets eaten by mice reported by Dorchies et al. (2006). However, according to Lambert et al. (2006a), different routes of EGCG administration lead to considerably different concentrations and half-lives of free EGCG in plasma. They found that oral or intragastric administration of 75 mg EGCG/kg body weight in mice gave a maximum plasma concentration of about 130 ng EGCG/ml and a half-life of just over an hour, whereas when EGCG is applied transdermally as a topical gel at a dose of 50 mg/kg body weight, its maximum plasma concentration is about 45 ng/ml, has a very much longer half-life of 94 h, and is mostly in a bioactive free form. In contrast, when EGCG is administered orally, most of it becomes methylated, glucuronidated and sulphated, thus reducing its bioavailability (Lambert et al. 2003; Lu et al. 2003). Assuming that there is an approximate linear relationship between dosage and plasma concentration (Lambert et al. 2006b), and that transdermal absorption yields approximately the same delivery dosage as subcutaneous injection, the subcutaneous administration
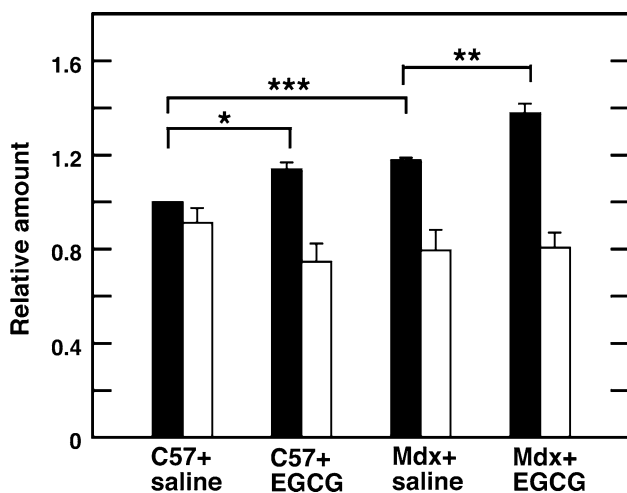
Fig. 10 Levels of utrophin protein and utrophin mRNA in diaphragm muscles in 8-week-old *mdx* and normal mice after treatment with EGCG or saline. These were determined as described in "Materials and methods". Each *column* and *bar* indicates the mean and SEM, respectively. The relative mean level (*black column*) of utrophin (taking that in C57 saline-treated mice as 1.0) was significantly higher by 18% in *mdx* saline-treated controls than in normal C57 controls. EGCG treatment increased the utrophin level significantly by 17 and 14% in *mdx* and C57 diaphragm muscles, respectively. In contrast, EGCG has no effect ($P > 0.2$, $P_B > 0.9$, $P_S > 0.6$) on the mean relative expression of utrophin mRNA (*white columns*) determined in diaphragm muscles in *mdx* and normal C57 mice using a quantitative real-time RT-PCR assay. * $P < 0.01$, * $P_B < 0.02$, * $P_S < 0.03$; ** $P < 0.01$, ** $P_B < 0.003$, ** $P_S < 0.004$; *** $P < 0.001$, *** $P_B < 0.005$, *** $P_S < 0.006$

of 5 mg EGCG/kg body weight employed in our experiments would give a fairly constant concentration of EGCG in the blood of roughly 4.5 ng/ml over 2–3 days. In contrast, if mice consumed 150 mg EGCG/kg body weight orally all at once, their plasma concentration would be approximately 260 ng/ml, about 60× higher than in our experiments, but the EGCG would be rapidly lost. In practice, mice would only eat on average about 6 mg EGCG/kg body weight per hour, corresponding to a plasma concentration of about 10 ng/ml, approximately twice the computed concentration in our study. However, in view of the approximations and assumptions underlying these calculations, the most that can be concluded is that the effective dose and bioavailability of EGCG in our experiments are of the same order as those yielded by the oral route employed by Ruegg and his colleagues (Dorchies et al. 2006), although subcutaneous administration allows a more precise control of the dosage in individual animals.

In their study, Dorchies et al. (2006) found that EGCG reduces the oxidative potential of the plasma in treated *mdx* mice, delayed muscle necrosis in the extensor digitorum longus, and improves quantitatively the functions of *mdx* triceps surae muscles. Our findings corroborate their observations. In contrast, these authors reported that the necrotic lesions in soleus muscles were not significantly reduced by

either EGCG or green tea extract administered orally to *mdx* mice for 1 or 5 weeks from the age of 3 weeks. However, as shown in the present study, subcutaneous injection of 5 mg/kg body weight EGCG into *mdx* mice for 8 weeks after birth significantly increased the relative percentage area of histologically normal muscle fibres and reduced that of necrotic muscle fibres (Figs. 5, 6), and prolonged the times of the maximum tetanic force of soleus muscles to fall by a half to almost normal levels (Fig. 7).

EGCG limited the onset of muscular dystrophy features more effectively in diaphragm muscle. Diaphragm muscle is a good one for studying the pathology of DMD (Stedman et al. 1991). We selected it not only for this reason but also because previously we found that the diaphragm muscles of *mdx* mice had already accumulated the products of oxidative damage, lipofuscin granules, by the time they were 4 weeks old (Nakae et al. 2004).

At present, one can only conjecture the different responses to EGCG of a slow-contracting muscle such as the soleus and a fast-contracting muscle such as the diaphragm reported here, or the soleus and extensor digitorum longus or triceps surae reported by Dorchies et al. (2006). One explanation proposed by these authors is that the different susceptibilities of the two muscle types may be partly due to their different fibre-type compositions. The mouse diaphragm and EDL consist entirely of fatiguable fast-twitch type II fibres (EDL, about 80% type IIB and 20% type IIX; Agbulut et al. 1996) whereas the soleus is mostly composed of type I fibres. Type IIB fibres appear to be more susceptible to cell death, presumably by free radicals such as $\cdot O_2$, than other fibre types (Rando 2002). If this is so, it is not surprising that muscles containing a preponderance of type IIB fibres are better protected by a free-radical scavenger or an antioxidant such as EGCG than muscles consisting mostly of type I fibres.

The significance of the increased amounts of utrophin that we observed after EGCG treatment is less clear. We observed that utrophin localises in a complex pattern to neuromuscular and myotendinous junctions, blood vessels, and peripheral nerves in mature normal and dystrophic muscles (Figs. 8, 9), confirming what others have reported previously (Khurana et al. 1991; Ohlendieck et al. 1991; Takemitsu et al. 1991; Clerk et al. 1993; Weir et al. 2002, 2004; Sewry et al. 2005). Utrophin is also strongly expressed in immature normal and dystrophic muscle cells along the entire length of their sarcolemma but the amount declines with maturation and ageing of muscle cells (Khurana et al. 1991; Takemitsu et al. 1991; Clerk et al. 1993; Sewry et al. 2005). This is illustrated in Figs. 8 and 9. We also observed that the level of utrophin is higher in mature *mdx* dystrophic muscles than in age-matched normal controls, illustrated in Figs. 8 and 10, and in agreement with previous reports (Gramolini et al. 1998; Weir et al. 2002,

2004). Our observations are the first evidence that EGCG treatment elevates utrophin levels on the extrasynaptic sarcolemma not only in dystrophic muscles but also in normal muscles. The increase in the utrophin levels is not due to muscle regeneration since *mdx* lingual muscles, which do not exhibit focal degeneration and regeneration at 8 weeks of age, also show this phenomenon (Fig. 9). The increased level persists considerably in mature muscle fibres in dystrophic muscles (Figs. 8, 9). However, the 17% increase in utrophin levels induced by EGCG that we observed in diaphragm muscle (Fig. 10) is modest, although significant ($P < 0.01$), and is smaller than that induced by heregulin (170% in tibialis anterior muscle, Krag et al. 2004) or by L-arginine (60% in diaphragm muscle, Voisin et al. 2005; 24% in EDL muscle, Barton et al. 2005). However, as EGCG does not elevate the steady-state utrophin mRNA levels in diaphragm muscles in *mdx* mice (Fig. 10), the higher levels of utrophin protein are not due to its enhanced expression. Further, as EGCG also significantly increases utrophin levels in diaphragm muscles of normal mice, by about 14%, 3% less than in the corresponding dystrophic muscle (Fig. 10), and the contraction properties of isolated normal soleus muscles are not significantly changed by our EGCG treatment regime (Fig. 7), the observed utrophin increases are not due to a specific stimulation by EGCG per se but are incidental.

In conclusion, our study corroborates other recent studies that EGCG is effective for limiting the onset of muscular dystrophy in newborn *mdx* mice without causing side effects, but the optimal dosage, administration route and the latest age at which treatment can be started in order to prevent muscle fibre necrosis and regeneration from occurring have still to be established. We are currently investigating whether EGCG has a beneficial effect when given to older mice when the myofibre necrosis–regeneration cycles have begun in earnest.

References

Agbulut O, Li Z, Mouly V, Butler-Browne GS (1996) Analysis of skeletal and cardiac muscle from desmin knock-out and normal mice by high resolution separation of myosin heavy-chain isoforms. Biol Cell 88:131–135

Barker T, Traber MG (2007) From animals to humans: evidence linking oxidative stress as a causative factor in muscle atrophy. J Physiol 583:421–422

Barton ER, Morris L, Kawana M, Bish LT, Toursel T (2005) Systemic administration of L-arginine benefits *mdx* skeletal muscle function. Muscle Nerve 32:751–760

Blake DJ, Weir A, Newey SE, Davies KE (2002) Function and genetics of dystrophin and dystrophin-related proteins in muscle. Physiol Rev 82:291–329

Buetler TM, Renard M, Offord EA, Schneider H, Ruegg UT (2002) Green tea extract decreases muscle necrosis in *mdx* mice and protects against reactive oxygen species. Am J Clin Nutr 75:749–753

Bulfield G, Siller WG, Wight PA, Moore KJ (1984) X chromosome-linked muscular dystrophy (*mdx*) in the mouse. Proc Natl Acad Sci USA 81:1189–1192

Burdi R, Didonna MP, Pignol B, Nico B, Mangieri D, Rolland JF, Camerino C, Zallone A, Ferro P, Andreetta F, Confalonieri P, De Luca A (2006) First evaluation of the potential effectiveness in muscular dystrophy of a novel chimeric compound, BN 82270, acting as calpain-inhibitor and anti-oxidant. Neuromuscul Disord 16:237–248

Chakkalakal JV, Thompson J, Parks RJ, Jasmin BJ (2005) Molecular, cellular, and pharmacological therapies for Duchenne/Becker muscular dystrophies. FASEB J 19:880–891

Clerk A, Morris GE, Dubowitz V, Davies KE, Sewry CA (1993) Dystrophin-related protein, utrophin, in normal and dystrophic human fetal skeletal muscle. Histochem J 25:554–561

Courdier-Fruh I, Barman L, Briguet A, Meier T (2002) Glucocorticoid-mediated regulation of utrophin levels in human muscle fibers. Neuromuscul Disord 12(Suppl 1):S95–S104

Dalkilic I, Kunkel LM (2003) Muscular dystrophies: genes to pathogenesis. Curr Opin Genet Dev 13:231–238

Disatnik MH, Dhawan J, Yu Y, Beal MF, Whirl MM, Franco AA, Rando TA (1998) Evidence of oxidative stress in *mdx* mouse muscle: studies of the pre-necrotic state. J Neurol Sci 161:77–84

Disatnik MH, Chamberlain JS, Rando TA (2000) Dystrophin mutations predict cellular susceptibility to oxidative stress. Muscle Nerve 23:784–792

Dorchies OM, Wagner S, Vuadens O, Waldhauser K, Buetler TM, Kucera P, Ruegg UT (2006) Green tea extract and its major polyphenol (-)-epigallocatechin gallate improve muscle function in a mouse model for Duchenne muscular dystrophy. Am J Physiol Cell Physiol 290:C616–C625

Dudley RWR, Danialou G, Govindaraju K, Lands L, Eidelman DH, Petrof BJ (2006) Sarcolemma damage in dystrophin deficiency is modulated by synergistic interactions between mechanical and oxidative/nitrosative stresses. Am J Pathol 168:1276–1287

Ervasti JM (2007) Dystrophin, its interactions with other proteins, and implications for muscular dystrophy. Biochim Biophys Acta 1772:108–117

Gerhardt W, Wulff K (1983) Creatine kinase. In: Bergmeyer HU (ed) Methods of enzymatic analysis. Verlag Chemie, Weinheim, pp 508–539

Goodin MG, Rosengren RJ (2003) Epigallocatechin gallate modulates CYP450 isoforms in the female Swiss-Webster mouse. Toxicol Sci 76:262–270

Gramolini AO, Burton EA, Tinsley JM, Ferns MJ, Cartaud A, Cartaud J, Davies KE, Lunde JA, Jasmin BJ (1998) Muscle and neural isoforms of agrin increase utrophin expression in cultured myotubes via a transcriptional regulatory mechanism. J Biol Chem 273:736–743

Hirst RC, McCullagh KJ, Davies KE (2005) Utrophin upregulation in Duchenne muscular dystrophy. Acta Myol 24:209–216

Khurana TS, Davies KE (2003) Pharmacological strategies for muscular dystrophy. Nat Rev Drug Discov 2:379–390

Khurana TS, Watkins SC, Chafey P, Chelly J, Tomé FM, Fardeau M, Kaplan JC, Kunkel LM (1991) Immunolocalization and developmental expression of dystrophin related protein in skeletal muscle. Neuromuscul Disord 1:185–194

Krag TO, Bogdanovich S, Jensen CJ, Fischer MD, Hansen-Schwartz J, Javazon EH, Flake AW, Edvinsson L, Khurana TS (2004) Heregulin ameliorates the dystrophic phenotype in *mdx* mice. Proc Natl Acad Sci USA 101:13856–13860

Lambert JD, Lee MJ, Lu H, Meng X, Hong JJ, Seril DN, Sturgill MG, Yang CS (2003) Epigallocatechin-3-gallate is absorbed but extensively glucuronidated following oral administration to mice. J Nutr 133:4172–4177

Lambert JD, Kim DH, Zheng R, Yang CS (2006a) Transdermal delivery of (-)-epigallocatechin-3-gallate, a green tea polyphenol, in mice. J Pharm Pharmacol 58:599–604

Lambert JD, Lee MJ, Diamond L, Ju J, Hong J, Bose M, Newmark HL, Yang CS (2006b) Dose-dependent levels of epigallocatechin-3-gallate in human colon cancer cells and mouse plasma and tissues. Drug Metab Dispos 34:8–11

Lu H, Meng X, Li C, Sang S, Patten C, Sheng S, Hong J, Bai N, Winnik B, Ho CT, Yang CS (2003) Glucuronides of tea catechins: enzymology of biosynthesis and biological activities. Drug Metab Dispos 31:452–461

Messina S, Altavilla D, Aguennouz M, Seminara P, Minutoli L, Monici MC, Bitto A, Mazzeo A, Marini H, Squadrito F, Vita G (2006) Lipid peroxidation inhibition blunts nuclear factor-κB activation, reduces skeletal muscle degeneration, and enhances muscle function in *mdx* mice. Am J Pathol 168:918–926

Miura P, Jasmin BJ (2006) Utrophin upregulation for treating Duchenne or Becker muscular dystrophy: how close are we? Trends Mol Med 12:122–129

Nakae Y, Stoward PJ, Shono M, Matsuzaki T (2001) Most apoptotic cells in *mdx* diaphragm muscle contain accumulated lipofuscin. Histochem Cell Biol 115:205–214

Nakae Y, Stoward PJ, Kashiyama T, Shono M, Akagi A, Matsuzaki T, Nonaka I (2004) Early onset of lipofuscin accumulation in dystrophin-deficient skeletal muscles of DMD patients and *mdx* mice. J Mol Histol 35:489–499

Nakae Y, Stoward PJ, Bespalov IA, Melamede RJ, Wallace SS (2005) A new technique for the quantitative assessment of 8-oxoguanine in nuclear DNA as a marker of oxidative stress. Application to dystrophin-deficient DMD skeletal muscles. Histochem Cell Biol 124:335–345

Nakae Y, Shono M, Stoward PJ (2006a) Assessment of oxidative stress in dystrophin-deficient dystrophic muscles of mice. Acta Anat Nippon 81(Suppl):214

Nakae Y, Hirasaka K, Goto J, Nikawa T, Shono M, Yoshida M, Stoward PJ (2006b) Subcutaneous injection of epigallocatechin gallate into dystrophin-deficient *mdx* mice ameliorates muscular dystrophy. In: Proceedings of the seventh joint meeting of the Histochemical Society and the Japanese Society of Histochemistry and Cytochemistry, p 156

Nakae Y, Hirasaka K, Goto J, Shono M, Yoshida M, Stoward PJ (2007) Subcutaneous injection of epigallocatechin gallate improves dystrophin-deficient muscular dystrophy in *mdx* mice and upregulates utrophin expression. Acta Anat Nippon 82:245

Narciso L, Fortini P, Pajalunga D, Franchitto A, Liu P, Degan P, Frechet M, Demple B, Crescenzi M, Dogliotti E (2007) Terminally differentiated muscle cells are defective in base excision DNA repair and hypersensitive to oxygen injury. Proc Natl Acad Sci USA 104:17010–17015

Ohlendieck K, Ervasti JM, Matsumura K, Kahl SD, Leveille CJ, Campbell KP (1991) Dystrophin-related protein is localized to neuromuscular junctions of adult skeletal muscle. Neuron 7:499–508

Pasquini F, Guerin C, Blake D, Davies K, Karpati G, Holland P (1995) The effect of glucocorticoids on the accumulation of utrophin by cultured normal and dystrophic human skeletal muscle satellite cells. Neuromuscul Disord 5:105–114

Passaquin AC, Metzinger L, Léger JJ, Warter JM, Poindron P (1993) Prednisolone enhances myogenesis and dystrophin-related protein in skeletal muscle cell cultures from *mdx* mouse. J Neurosci Res 35:363–372

Rando TA (2002) Oxidative stress and the pathogenesis of muscular dystrophies. Am J Phys Med Rehabil 81:S175–S186

Rando TA, Disatnik MH, Yu Y, Franco A (1998) Muscle cells from *mdx* mice have an increased susceptibility to oxidative stress. Neuromuscul Disord 8:14–21

Sewry CA, Nowak KJ, Ehmsen JT, Davies KE (2005) A and B utrophin in human muscle and sarcolemmal A-utrophin associated with tumours. Neuromuscul Disord 15:779–785

Stedman HH, Sweeney HL, Shrager JB, Maguire HC, Panettieri RA, Petrof B, Narusawa M, Leferovich JM, Sladky JT, Kelly AM (1991) The *mdx* mouse diaphragm reproduces the degenerative changes of Duchenne muscular dystrophy. Nature 352:536–539

Takemitsu M, Ishiura S, Koga R, Kamakura K, Arahata K, Nonaka I, Sugita H (1991) Dystrophin-related protein in the fetal and denervated skeletal muscles of normal and *mdx* mice. Biochem Biophys Res Commun 180:1179–1186

Tidball JG, Wehling-Henricks M (2007) The role of free radicals in the pathophysiology of muscular dystrophy. J Appl Physiol 102:1677–1686

Voisin V, Sébrié C, Matecki S, Yu H, Gillet B, Ramonatxo M, Israël M, De la Porte S (2005) L-arginine improves dystrophic phenotype in *mdx* mice. Neurobiol Dis 20:123–130

Weir AP, Burton EA, Harrod G, Davies KE (2002) A- and B-utrophin have different expression patterns and are differentially up-regulated in *mdx* muscle. J Biol Chem 277:45285–45290

Weir AP, Morgan JE, Davies KE (2004) A-utrophin up-regulation in *mdx* skeletal muscle is independent of regeneration. Neuromuscul Disord 14:19–23

Williams IA, Allen DG (2007) The role of reactive oxygen species in the hearts of dystrophin-deficient *mdx* mice. Am J Physiol Heart Circ Physiol 293:H1969–H1977

Xiao X, Li J, Tsao YP, Dressman D, Hoffman EP, Watchko JF (2000) Full functional rescue of a complete muscle (TA) in dystrophic hamsters by adeno-associated virus vector-directed gene therapy. J Virol 74:1436–1442

Zaccagnini G, Martelli F, Magenta A, Cencioni C, Fasanaro P, Nicoletti C, Biglioli P, Pelicci PG, Capogrossi MC (2007) p66(ShcA) and oxidative stress modulate myogenic differentiation and skeletal muscle regeneration after hind limb ischemia. J Biol Chem 282:31453–31459